

# NUMERICAL STUDY ON DIFFUSION IN A ROOM WITH A LOCALLY BALANCED SUPPLY-EXHAUST AIRFLOW RATE SYSTEM

S. Kato, D.Eng.  
Member ASHRAE

S. Murakami, D.Eng.  
Member ASHRAE

S. Nagano

## ABSTRACT

Flow and diffusion fields in rooms are studied by means of numerical simulation. The rooms used are models of conventional flow-type clean rooms. In the rooms, the exhaust as well as the supply openings are set in the ceiling. The exhaust openings are installed so that the supply and exhaust airflow rates are balanced locally in that space. This ventilation system is intended to avoid formation of a large recirculating flow in the whole room. The flow field is composed of series of "flow units" in which supply-exhaust flows are locally "confined" and "closed off" from other units. Each flow unit consists of a supply jet and the rising recirculating streams around it. This locally confined flow field is effective in limiting diffusion of contaminants to within a local area, compared with conventional methods.

Numerical simulation is performed for the following four cases: (1) supply and exhaust airflow rates are locally balanced for each flow unit, (2) supply and exhaust airflow rates are set to agree with the results of a model experiment, (3) a flow obstacle is arranged, and (4) a balance between the supply and exhaust airflow rates for one flow unit is not maintained. Supply and exhaust airflow rates can be set more exactly in numerical simulation than in experiments or actual trials. Therefore, precise examination of the effects of an imbalance between supply and exhaust rates can be conducted quantitatively only by means of numerical simulation. The ventilation efficiency of the room was quantitatively examined using the scale of ventilation efficiency (SVE 1-3) proposed earlier by the authors, based on the results of numerical study.

## INTRODUCTION

Installing both supply and exhaust openings in the ceiling of a room may be considered an effective design for industrial buildings where production lines are often changed in accord with changes in production. In this context, the characteristics of a ventilation system where both supply and exhaust openings are set in the ceiling must be clarified.

The authors have analyzed the characteristics of flow and diffusion fields systematically in conventional flow-type clean rooms in preceding papers (Murakami et al. 1987, 1988, 1989, 1990a) as follows:

1. The airflow pattern in a conventional clean room that has supply openings in the ceiling can be modeled as a serial combination of "flow units," which consist of one supply jet and the rising flow around it, as shown in Figure 1.
2. The exhaust does not have a significant effect on the total airflow pattern.
3. The diffusion field of the contaminant can be analyzed well using flow units, which can be modeled separately. The contaminant is diffused first within the flow unit, where it is generated before being convected into other flow units toward the exhaust.
4. The diffusion characteristics of the contaminant are significantly affected by the positions of the exhaust openings relative to the serial combination field of these flow units.

By expanding on this concept of flow units, a ventilation system based on the concept of locally balanced supply-exhaust airflow, in which the air supply and

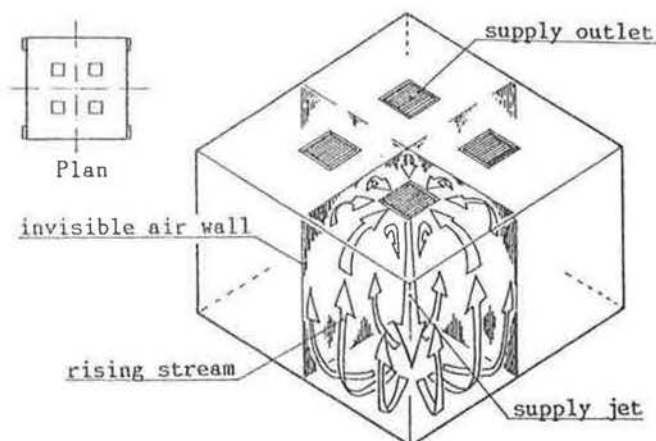


Figure 1 Concept of flow unit.

Shinsuke Kato is an associate professor and Shuzo Murakami is a professor at the Institute of Industrial Science, University of Tokyo, Japan. Shin-ichiro Nagano is a researcher at the Technical Research Institute, Fujita Corporation, Japan.

THIS PREPRINT IS FOR DISCUSSION PURPOSES ONLY, FOR INCLUSION IN ASHRAE TRANSACTIONS 1992, V. 98, Pt. 1. Not to be reprinted in whole or in part without written permission of the American Society of Heating, Refrigerating, and Air-Conditioning Engineers, Inc., 1791 Tullie Circle, NE, Atlanta, GA 30329. Opinions, findings, conclusions, or recommendations expressed in this paper are those of the author(s) and do not necessarily reflect the views of ASHRAE. Written questions and comments regarding this paper should be received at ASHRAE no later than Feb. 7, 1992.

exhaust are matched for each flow unit, makes it possible to confine the diffusion of contaminants to the flow unit where they are generated. From the practical viewpoint of the duct system, such a system can be realized when both the supply and exhaust openings are set in the same plane, such as the ceiling. The authors think this is a highly effective design for contamination control in a room, especially in a conventional flow-type clean room. Thus, this paper will examine the flow and diffusion fields of clean rooms having this ventilation system in the ceiling.

Currently there are several systems that handle air supply and exhaust in the ceiling; such systems are common in office buildings. However, the flow and diffusion fields of such systems have not yet been examined thoroughly, and, in particular, none is designed on the basis of locally balanced supply-exhaust airflow rates. From the viewpoint of ordinary contamination control in a clean room, particular concerns that arise for this system are as follows.

1. Contaminants generated near the floor are convected toward the ceiling by the rising stream; hence, they are exhausted only after rising to the ceiling. This is inconsistent with the principle of immediate contaminant exhaust.
2. A short circuit may be formed between the supply and the exhaust flows when the inlet and outlet are set close together. This may create a stagnant flow region in which the contaminant is not exhausted effectively. To confirm that such a short circuit does not occur and that setting the exhaust in the ceiling does not reduce ventilation efficiency for exhausting contaminant, the authors examined the flow and diffusion fields of ventilation systems having locally balanced supply-exhaust airflow in the ceiling by means of numerical simulation and tested the effectiveness of such a system in contamination control.

As shown in the appendix, the flow and diffusion fields of this type of room were analyzed earlier in model experiments. The results confirmed that a ventilation system using locally balanced supply-exhaust airflow is an effective means of controlling contaminant diffusion if a local air balance is attained for each flow unit. However, it proved difficult to examine the characteristics of flow and diffusion fields quantitatively in detail using model experiments because of the many disturbances arising from the experimental conditions. On the other hand, the authors have previously shown that a numerical simulation based on the  $k-\epsilon$  turbulence model is a reliable predictor of the characteristics of complex three-dimensional flow fields if sufficient care is taken in the calculation procedure, even though small problems remain to be solved (Murakami et al. 1987, 1988).

In the numerical simulation, the supply and exhaust flow rates can be precisely controlled, and it is possible to analyze the effects of various factors on the diffusion

fields. It is also possible to apply quantitative methods to the distribution of ventilation efficiency in the clean room by means of SVE 1-3 as proposed by the authors (Kato and Murakami et al. 1988; Murakami et al. 1988).

## ROOM MODELS ANALYZED

The flow and diffusion fields in rooms with nine supply outlets, as shown in Figure 2, were analyzed. These rooms are models of conventional flow-type clean rooms.

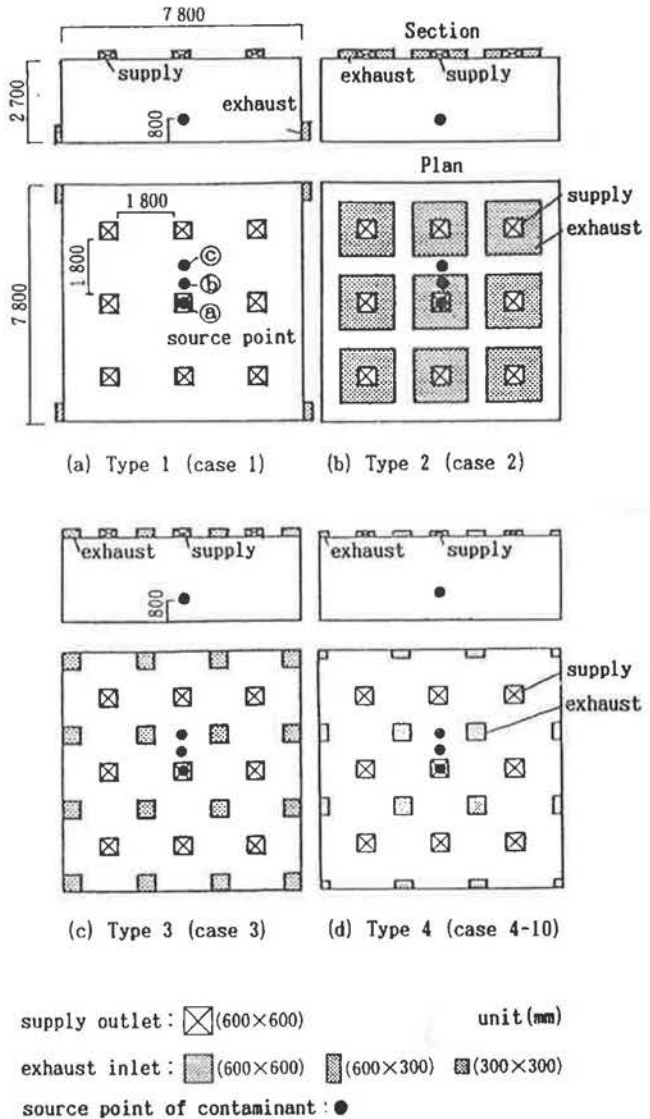


**Figure 2** Configurations of model clean rooms and layouts of supply-exhaust openings. Type shows the different layouts of supply-exhaust openings. Case refers to differences in the simulation conditions. (In cases 5 through 10, source is located only at position @. It is just under the supply jet in the center of the room.)

Type 1 (conventional-style wall exhaust) has an exhaust mode in which four exhaust openings are located in the wall near the floor; Types 2 through 4 are varieties of the locally balanced supply-exhaust airflow system in the ceiling. Type 2 has a layout with exhaust inlets around each supply outlet, while Types 3 and 4 have layouts in which the outlets and inlets are laid out in a diamond pattern. In Type 2, the exhaust inlets are arranged so as to exhaust the convergent flow along the ceiling toward the supply outlets in each flow unit before it is induced by the supply jet. In Types 3 and 4, they are placed so as to catch the rising streams at the ceiling, where they are strongest in each flow unit. In Type 3, the areas of all exhaust openings are the same and the exhaust rate is adjusted by varying the exhaust velocity in order to attain a local air balance, while in Type 4 the exhaust velocity is kept constant for all openings and the area of the opening is changed. The sources of contaminants in the simulated diffusion fields are shown by black dots with (a), (b), and (c).

### CASES ANALYZED

Table 1 shows the various cases of simulations performed. For a constant air supply rate of 70 air changes per hour (the Reynolds number of supply jets is 40,000), the four types of exhaust inlet designs (cases 1 through 4) were compared. Next, the effect of flow obstacles was examined using a Type 4 room model (cases 5 and 6). The effect of placing obstacles at (a), just under the supply outlet in the center of the room (case 5), and at (b), just under the exhaust inlet (case 6), was examined, as shown in Figure 3. Figure 4 shows the air velocity at the supply and exhaust openings for each case. To examine the effect of changes in the airflow rate distribution for supply and exhaust openings, four cases, 7 through 10, were examined with regard to the Type 4 room model, as shown in Figures 4e through 4h.

### NUMERICAL METHOD

Three-dimensional numerical simulations were carried out on the basis of the  $k-\epsilon$  two-equation model. The governing equations are shown in Table 2, and the boundary conditions and the finite difference scheme are shown in Table 3. The numerical procedure adopted here was described in detail in Murakami et al. (1987).

The concentration distribution of contaminants was analyzed using the transport equation (Equation 6 of Table 2) based on the distribution of velocity and the eddy viscosity coefficient after calculating the flow field. In the diffusion calculation, it was assumed that contaminants were generated at a discharging velocity of zero and were assumed to be passive scalar contaminants, disregarding effects such as gravitational sedimentation. The rate of generation was set so that the perfect mixing concentration

equaled one (in other words, concentration is expressed as a dimensionless value by dividing by the perfect mixing concentration, which is identical to the averaged concentration at exhaust openings), and the stationary solution was calculated. The model room used in the analyses was divided into uniform meshes (0.15 m per side). Figure 5 shows the mesh divisions in the case of a Type 4 model. In all cases, the room was divided into  $54(x) \times 54(y) \times 22(z)$  cells. The simulated results of airflow distribution show small fluctuations in space and time, and the symmetry of the concentration distribution was not fully satisfied in response to the asymmetry of the flow field.

### METHODS OF EXPRESSING CONTAMINANT DIFFUSION FIELDS AND DEFINITION OF SVE 1-3

In this study, contaminant diffusion fields are expressed by four methods:

1. Distribution of contaminant concentration in the case of a point source. This distribution allows intuitive comprehension of the contaminant diffusion fields in a room.
2. Spatial average concentration—the first scale of ventilation efficiency (SVE 1). This value is proportional to the average time the contaminants are present in the room and indicates how quickly the contaminants generated in the room are exhausted by the flow field.
3. Mean radius of diffusion—the second scale of ventilation efficiency (SVE 2). This value represents the average spatial diffusion.

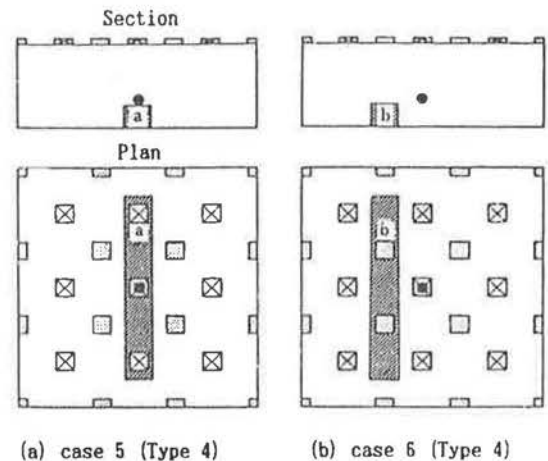


Figure 3 Arrangement of obstacle.

**TABLE 1**  
**Specifications of Analysis**

Item for analysis	Simulation Case	Type of room mold	Obstacle	Local air balance or imbalance	Figures	Remarks
Layout of supply and exhaust openings	Case 1	Type 1	Nothing	Balanced	Figure 8 Figure 13	Contaminants generated at three points, ① through ③ Contaminants generated uniformly throughout the whole room
	Case 2	Type 2	Nothing	Balanced	Figure 9	Contaminants generated at three points, ① through ③
	Case 3	Type 3	Nothing	Balanced	Omitted (same as Figure 10)	Contaminants generated at three points, ① through ③
	Case 4	Type 4	Nothing	Balanced	Figure 10 Figure 14	Contaminants generated at three points, ① through ③ Contaminants generated uniformly throughout the whole room
Flow obstacle	Case 4	Type 4	Nothing	Balanced	Figure 10	
	Case 5	Type 4	Position ①	Balanced	Figure 15	Contaminants generated only at point ①
	Case 6	Type 4	Position ②	Balanced	Figure 16	Contaminants generated only at point ②
Local air balance or imbalance	Case 4	Type 4	Nothing	Balanced	Figure 10	
	Case 7	Type 4	Nothing	Corresponding to experiment	Figure 6 Figure 7	Results of model experiment Two types of contaminant generation at supply outlet and point ①
	Case 8	Type 4	Nothing	Imbalanced *1	Figure 17	Contaminant generated only at point ①
	Case 9	Type 4	Nothing	Imbalanced *2	Figure 18	Contaminant generated only at point ①
	Case 10	Type 4	Nothing	Balanced *3	Figure 19	Contaminant generated only at point ①

NOTE : \*1 Reduced air volume rate at supply outlet in the center of room  
 \*2 Increased air volume rate at supply outlet in the center of room  
 \*3 Increased air volume rate at the center "flow unit" (air flow rate both at the center supply outlet and the surrounding exhaust inlets are increased)  
 \*4 Air exchange rate is the same value (70 per hour) except case 7 (66 per hour).



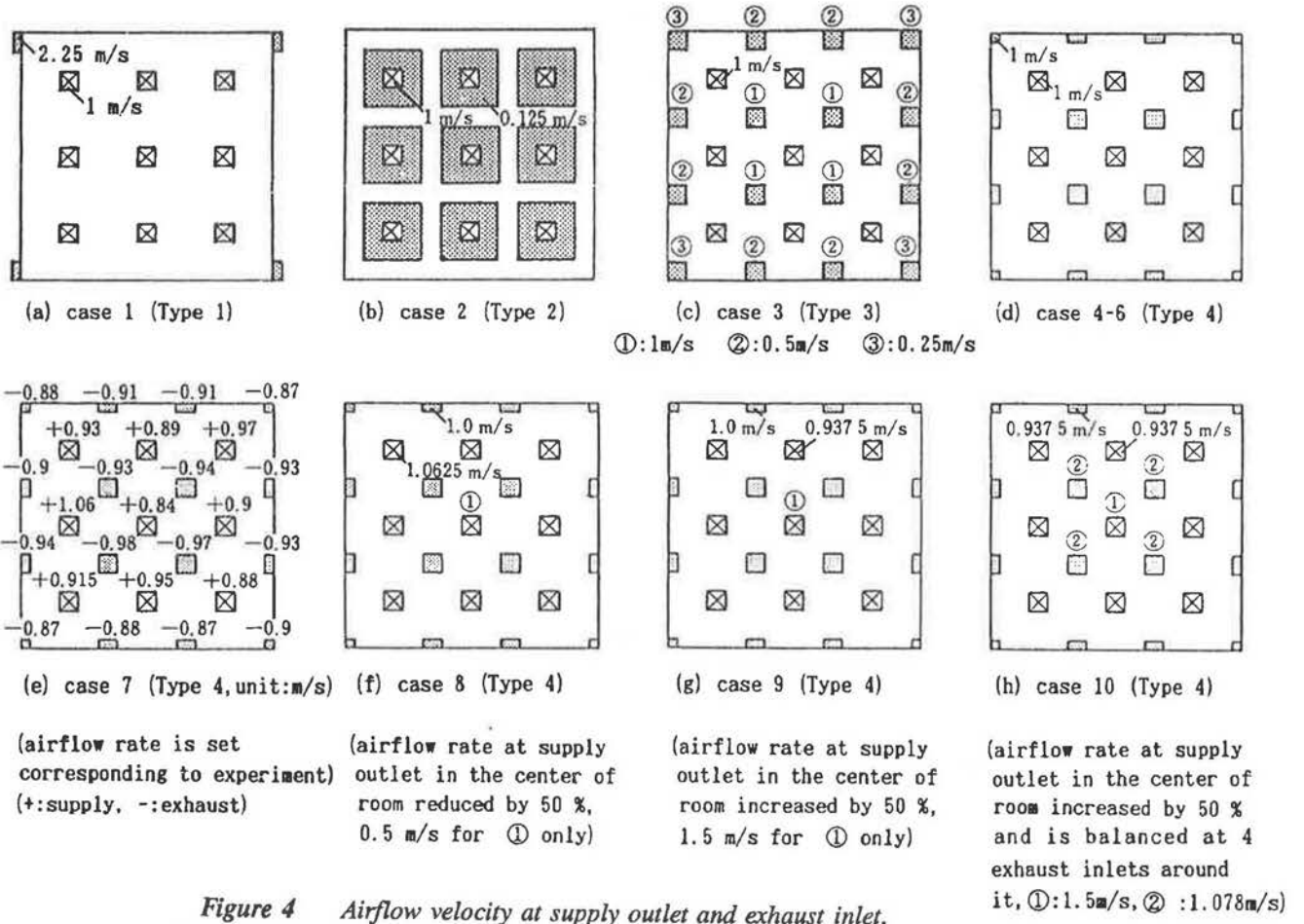


Figure 4 Airflow velocity at supply outlet and exhaust inlet.

TABLE 2  
k-ε Two-Equation Turbulence Model

---

(1) Continuity equation

$$\frac{\partial U_i}{\partial X_i} = 0$$

(2) Momentum equations

$$\frac{\partial U_i}{\partial t} + \frac{\partial U_i U_j}{\partial X_j} = - \frac{\partial}{\partial X_i} \left( \frac{P}{\rho} + \frac{2}{3} k \right) + \frac{\partial}{\partial X_j} \left\{ \nu_t \left( \frac{\partial U_i}{\partial X_j} + \frac{\partial U_j}{\partial X_i} \right) \right\}$$

(3) Transport equation for turbulent energy k

$$\frac{\partial k}{\partial t} + \frac{\partial k U_j}{\partial X_j} = \frac{\partial}{\partial X_j} \left( \frac{\nu_t}{\sigma_k} \frac{\partial k}{\partial X_j} \right) + \nu_t S' - \epsilon$$

(4) Transport equation for turbulent energy dissipation ε

$$\frac{\partial \epsilon}{\partial t} + \frac{\partial \epsilon U_j}{\partial X_j} = \frac{\partial}{\partial X_j} \left( \frac{\nu_t}{\sigma_\epsilon} \frac{\partial \epsilon}{\partial X_j} \right) + C_1 \frac{\epsilon}{k} \nu_t S' - C_2 \frac{\epsilon^2}{k}$$

(5) Expression of eddy kinematic viscosity based on eddy viscosity modelling

$$\nu_t = C_\mu \frac{k^2}{\epsilon} = C_\mu \frac{k}{\varrho}$$

(6) Transport equation for concentration C

$$\frac{\partial C}{\partial t} + \frac{\partial C U_j}{\partial X_j} = \frac{\partial}{\partial X_j} \left( \frac{\nu_t}{\sigma_c} \frac{\partial C}{\partial X_j} \right) + C_s$$

Here,  $S' = 2 S_{11} S_{11} = 2 \left\{ \frac{1}{2} \left( \frac{\partial U_i}{\partial X_j} + \frac{\partial U_j}{\partial X_i} \right) \right\}^2$

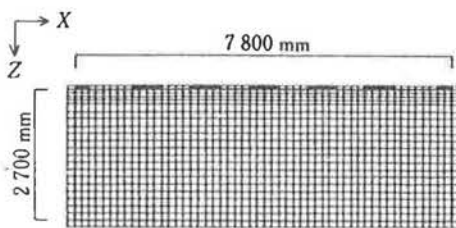
$$\sigma_1 = 1.0, \sigma_2 = 1.3, \sigma_3 = 1.0, C_\mu = 0.09, C_1 = 1.44, C_2 = 1.92$$


---

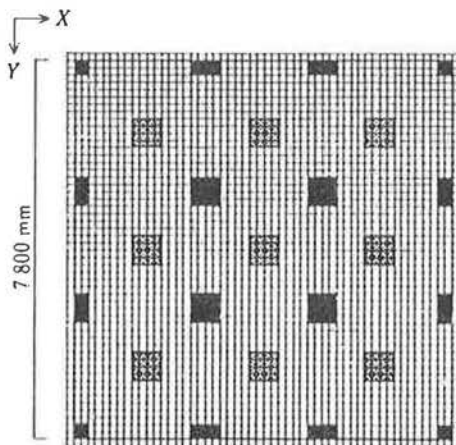
**TABLE 3**  
**Boundary Conditions and Finite Difference Scheme**





(1) Supply Outlet	$U_t=0.0, U_n=U_{out}, k_o=0.005(m^2/s^2), \ell_o=0.3(m), C=0.0$ subscript t, n: tangential and normal direction with respect to outlet surface. $U_{out}$ : supply outlet velocity (=1.0 m/s) $k_o$ : kinematic energy given at supply outlet $\ell_o$ : length scale of turbulence given at supply outlet
(2) Exhaust Inlet	$U_t=0.0, U_n=U_{in}, \partial k/\partial n=0.0, \partial \epsilon/\partial n=0.0, \partial C/\partial n=0.0$ $U_{in}$ : exhaust inlet velocity (=1.0 m/s)
(3) Wall Surface	$(\partial U_t/\partial n)_{n=0}=m(U_t)_{n=h}/h, U_n=0.0, \partial k/\partial n=0.0, \partial C/\partial n=0.0,$ $(\epsilon)_{n=h}=(C\mu k_{n=h}^{3/2})/(C\mu^{1/4}\kappa h)$ h: distance from wall surface to the center of the near-wall cell m: 1/7, power law profile $U_t \propto Z^m$ is assumed near the wall $\kappa$ : 0.4, von Karman constant
(4) Finite Difference Scheme	Space differential: 1) QUICK scheme : transport equations for k, $\epsilon$ and velocity 2) First-order upwind scheme : transport equation for C 3) Centered differential scheme for all others Time differential: Adams-Bashforth scheme with second-order accuracy

NOTE: This simulation is performed using full-scale physical parameters.



(a) Vertical section  
: 54 (X) x 22 (Z) meshes



(b) Horizontal section  
: 54 (X) x 54 (Y) meshes  
 supply outlet :   
 exhaust inlet :   

- Concentration in case of uniform contaminant generation throughout the room—the third scale of ventilation efficiency (SVE 3). At a given point, this value is proportional to the mean traveling time of the supply air to that point. A high value for this concentration indicates a high possibility of air contamination because the air mass must have traveled a long way from the supply outlet.

The details of these scales are described in Kato and Murakami (1988).

#### COMPARISON OF MODEL EXPERIMENT WITH THE SIMULATION

Figure 6 shows the results of experiments performed under conditions corresponding to those of a Type 4 room model. These results are summarized in the appendix. Figure 7 shows the simulation results of Type 4 in which the airflow rate values for each outlet and inlet are given as measured in the experiments (case 7). Generally, the speed and direction of the rising airstreams between supply outlets and the airstream rising up along the wall agree well with the experimental results (Figures 6a and 7a). Although the simulation reproduces less velocity where the supply jet strikes the floor, the difference from the experiment is small. While experimental measurements of diffusion fields have agreed relatively well with simulations in past studies (Murakami et al. 1987, 1988), some differences can be found in this case. First, while a domain of concentration lower than 0.5 appeared at the wall in the simulation, it was not observed in the experiment. Second, with regard to high-concentration

Figure 5 Mesh dividing system (Type 4). (Mesh system is the same for all types.)

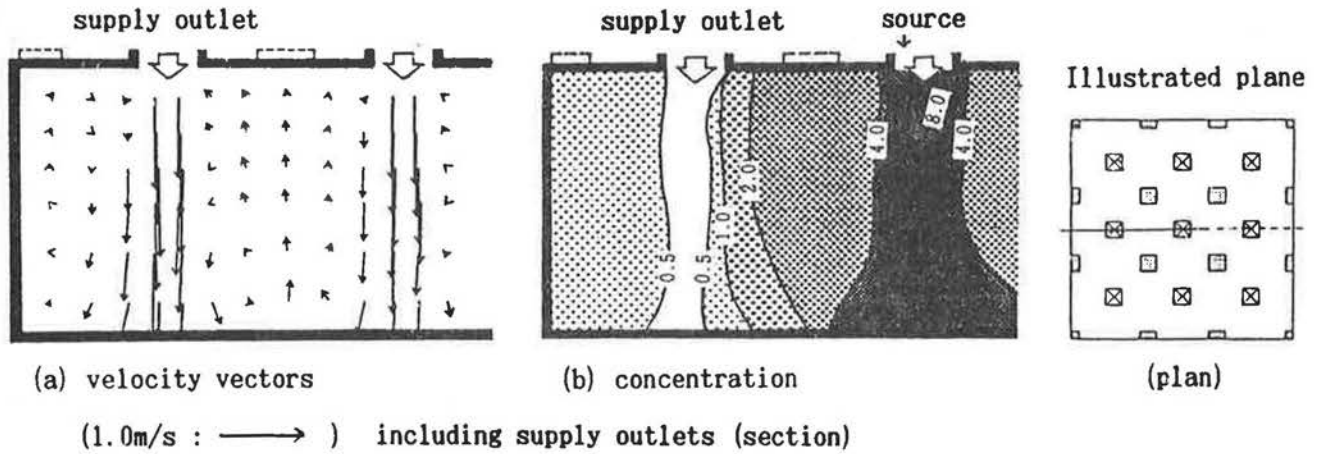


Figure 6 Experimental results of velocity vectors and contaminant distribution in case 7. (Room model: Type 4, contaminant injected at supply outlet in the center of room.)

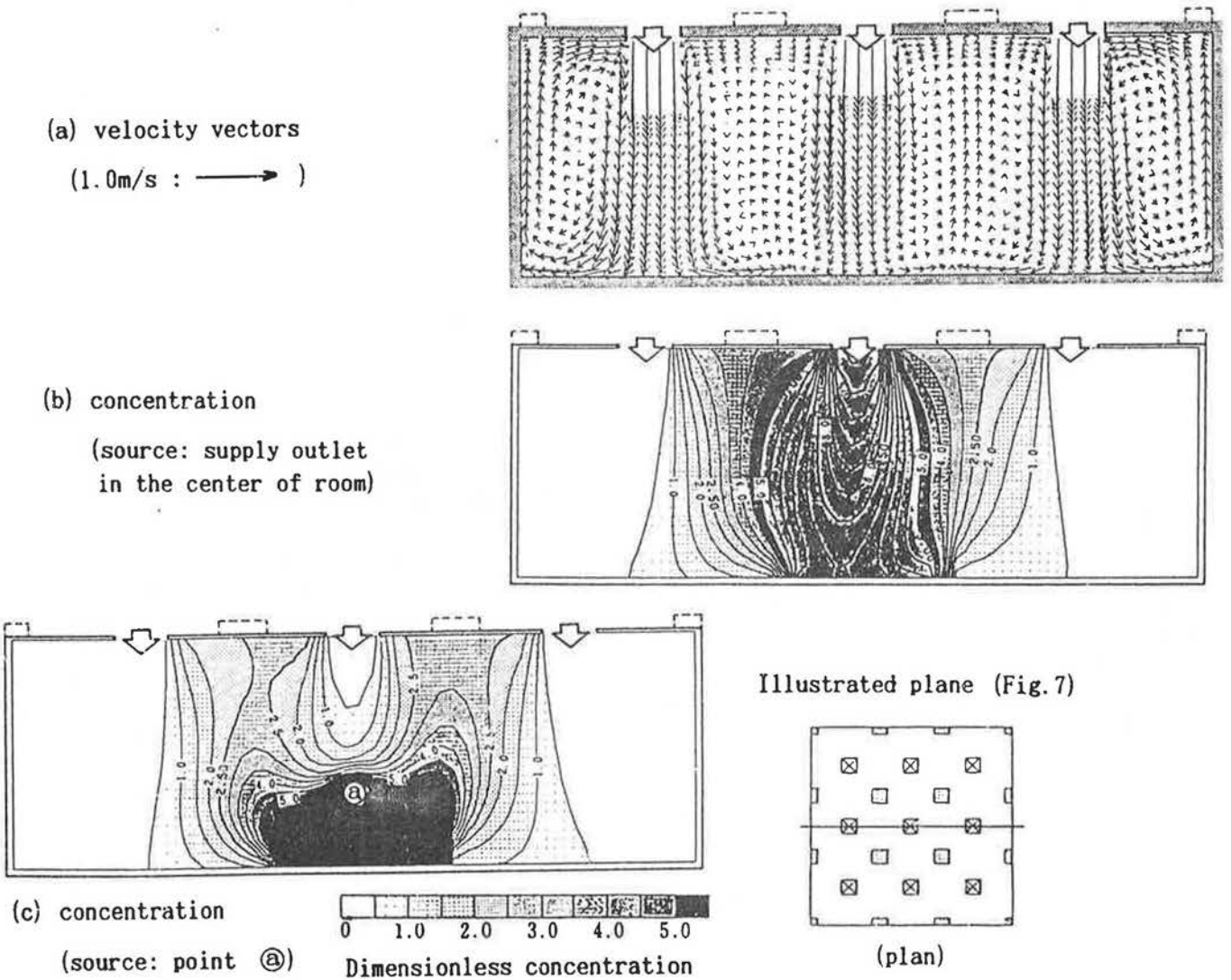


Figure 7 Velocity vectors and contaminant distribution in case 7. (Room model: Type 4, simulation. In this case, the airflow rate at each supply and exhaust is not uniform and varies according to its measured value in the experiment.)

domains over 2, the simulation yielded slightly higher values than those in the model experiments (Figures 6b and 7b). The diffusion fields estimated by simulation this time generally showed less diffusion than did the experiments. The difference is caused partly by small discrepancies in the flow conditions between simulations and experiments. In other words, it is difficult to precisely measure the flow conditions at the supply and exhaust openings in the experiments, and therefore it is also difficult to thoroughly reflect these circumstances in the simulations. It might be noted that, from the viewpoint of turbulent flow theory, the eddy diffusivity model, which is used in the  $k-\epsilon$  turbulence model, is not precise enough to reproduce the turbulent scalar diffusion field (e.g., Murakami et al. 1990b). However, the primary purpose of this work was to parametrically compare the effects of supply-exhaust flow rate distribution and obstacles on the flow fields. In this sense, confirmation of a correspondence between this simulation technique and the experimental results means that the method is definitely effective for this purpose.

Figure 7c shows the simulation for the case when contaminants are generated at point (a). The diffusion characteristics are generally similar to those when contaminants are generated at the supply outlets, as shown in Figure 7b. It can be seen that although the contaminant distribution in the flow unit is greatly affected by the position of the generation source in the flow unit, the effect of contaminant generation on other flow units is extremely small. This matter will be examined again later.

#### EFFECT OF CHANGES IN POSITION AND SHAPE OF EXHAUST INLETS (COMPARISON BETWEEN TYPES 1-4)

Figures 8a, 9a, and 10a show the flow fields of case 1 (Type 1, exhaust in the wall) and cases 2 and 4 (Types 2 and 4, locally balanced supply-exhaust airflow system in the ceiling). Because the airflow patterns of case 3 (Type 3) and case 4 (Type 4) are similar due to the same airflow rate at each opening and the similar layout of the openings, a description of case 3 (Type 3) is omitted. The airflow patterns agree well with the results of the model experiments (cf. appendix). While with Type 1 the rising airflow between supply outlets came to a standstill at a point about two-thirds of the height from the floor without reaching the ceiling (Figure 8a), in Types 2 through 4 the rising airflow reached the ceiling (Figures 9a and 10a). On the whole, the local airflow patterns of Types 2 through 4 are affected to a small degree by differences in the arrangement of exhaust inlets, but the general airflow patterns in the entire space are very similar. In all cases, the discharged jet diverges after striking the floor, and the diverging airflow reaches the wall or collides with another to form a rising airstream that encloses the jet; after the rising flow reaches the ceiling, the flow converges along

the ceiling. This flow pattern for one supply opening forms a flow unit, as shown in Figure 1. The total airflow pattern in a room appears to consist of a series of those flow units, each possessing a supply jet in its center.

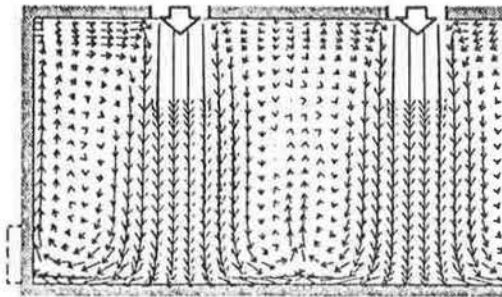
#### CHARACTERISTICS OF CONTAMINANT DIFFUSION (IN THE CASE OF A POINT SOURCE)

Figures 8 through 10, parts b and c, show contaminant diffusion fields for cases 1, 2, and 4 (Types 1, 2, and 4) in the case where contaminants are generated at point (a), 0.8 m above the floor in the center of the room (just under the center supply outlet). The diffusion fields of case 3 (Type 3) are not shown, as they resemble those of Case 4. As stated before, while the general airflow patterns of Type 1 (exhausts set in the wall) and Types 2 through 4 (locally balanced supply-exhaust airflow rate system in the ceiling) resemble each other, their contaminant diffusion fields are extremely different. In the case of Types 2 through 4 (Figures 9 and 10), where both supply and exhaust are arranged in the same flow unit, the diffusion of contaminants is basically confined and limited to that flow unit and its immediate vicinity, as though an invisible air boundary limits the diffusion of contaminants. For this reason, the diffusion fields of Types 2 through 4 differ significantly from that of Type 1, where contaminants diffuse widely throughout the room (Figure 8). The diffusion in the case of Type 2 becomes a little wider in the lower part of the room compared with Types 3 and 4.

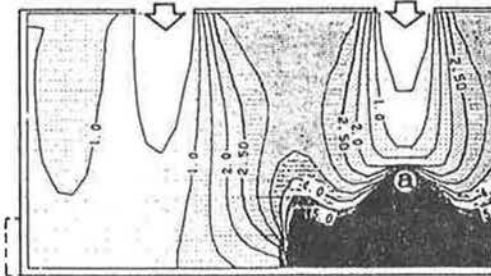
#### FEATURES OF SVE 1 (AVERAGE CONCENTRATION IN THE ROOM) AND SVE 2 (CONTAMINANT DIFFUSION RADIUS)

Figures 11 and 12 show SVE 1 and SVE 2 (average concentration in the room and average diffusion radius of contaminants, respectively) in cases where the source of contaminants is moved to points (b) and (c) from point (a) for each case (Figure 2). Table 4 shows the values of SVE 1 and SVE 2 in each case. Considering SVE 1 in Figure 11, cases 2 through 4 (Types 2 through 4) exhibit values about half those in case 1 (Type 1), when the source is at (a). SVE 1 corresponds to the average staying time of contaminants before being exhausted from the room and, in the case of the local air balance system of cases 2 through 4 (Types 2 through 4), it can be seen that the average staying time is about half that of case 1 (Type 1), which suggests that the exhaust efficiency is significantly higher. Also, as shown in Figure 12, SVE 2 indicates that with case 1 (Type 1) there is much more diffusion of contaminants throughout the room than with cases 2 through 4 (Types 2 through 4). The diffusion radius becomes smaller as the source moves from point (a)



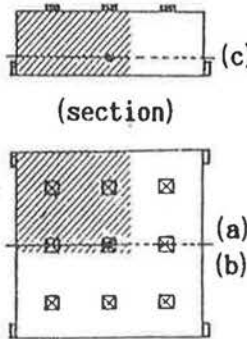


(a) velocity vectors

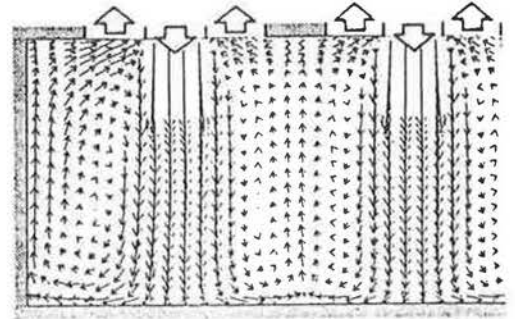


(b) concentration including supply outlets (section)

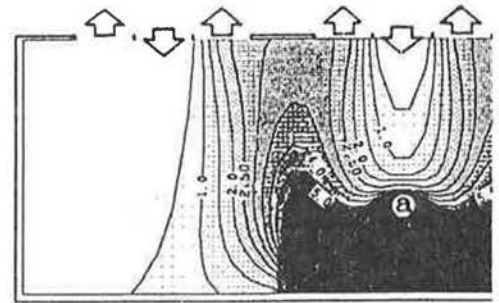
Illustrated plane (Fig. 8)



(plan)

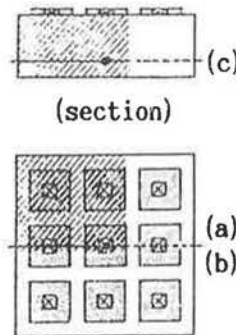


(a) velocity vectors

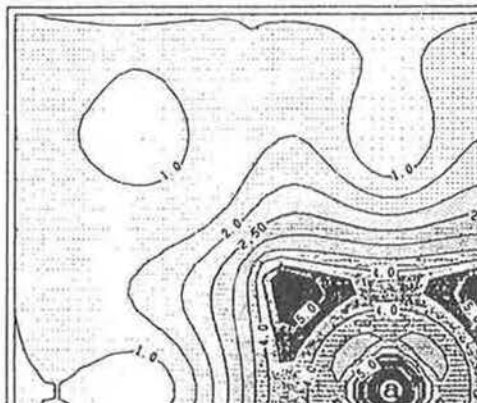


(b) concentration including supply outlets (section)

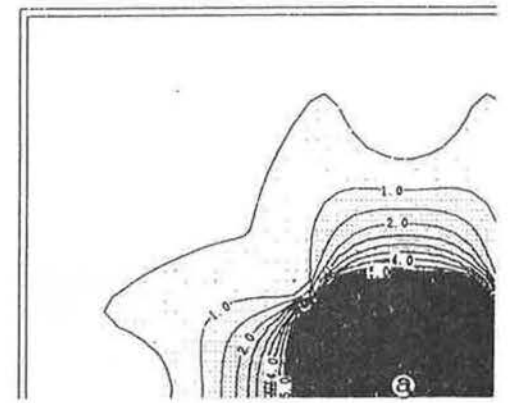
Illustrated plane (Fig. 9)



(plan)



(c) concentration 0.8m above floor (plan)



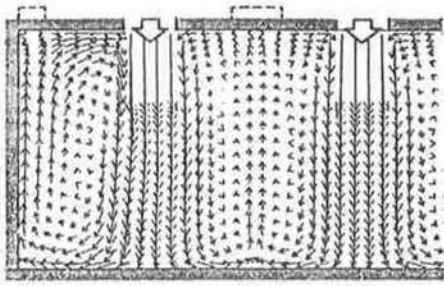
(c) concentration 0.8m above floor (plan)

**Figure 8** Velocity vectors and contaminant distribution in case 1. (Type 1, simulation, source: point  $\textcircled{a}$ .)

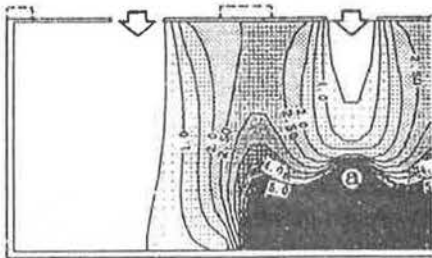
**Figure 9** Velocity vectors and contaminant distribution in case 2. (Type 2, simulation, source: point  $\textcircled{a}$ .)

in the center of the room to point  $\textcircled{c}$  between the supply outlets. The reason for this is that diffusion is progressively limited as the source moves closer to the exhaust downstream in each flow unit. In cases 2 through 4 (Types 2 through 4), because source  $\textcircled{a}$  is in the supply jet, which is located relatively upstream in each flow unit, contaminants become thoroughly diffused within each flow unit. On the other hand, compared with point  $\textcircled{a}$ ,  $\textcircled{c}$  is located in a rising airstream, relatively close to the exhaust inlet in each flow unit. Since the contaminants are

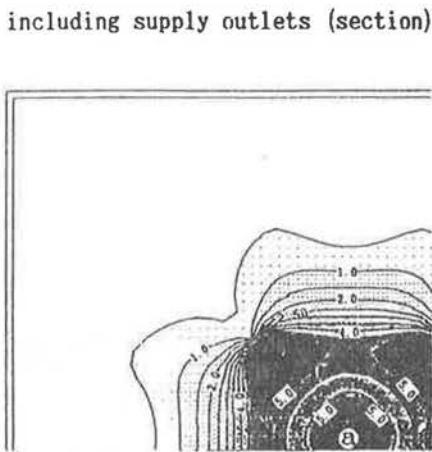
transported to the ceiling by the rising airstream and are efficiently exhausted through the exhaust flow before diffusing into the room, the value of the diffusion radius is much smaller. With Type 2, the values of SVE 1 and SVE 2 are larger than with Types 3 and 4, so the ventilation efficiency is lower. In Types 3 and 4, the rising airstream becomes strongest, since it directly faces the exhaust inlets (the stream rises directly toward the exhaust inlet) and this is thought to be one reason why the ventilation efficiency is higher.



(a) velocity vectors



(b) concentration



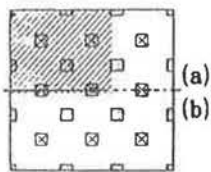
(c) concentration

0.8m above floor (plan)

Illustrated plane  
(Fig. 10)



(section)



(plan)

(a)

(b)

Figure 10 Velocity vectors and contaminant distribution in case 4. (Type 4, simulation, source: point @.)

- point @ : center of room
- △ point ⑥ : near supply outlet
- point ③ : center between supply outlets

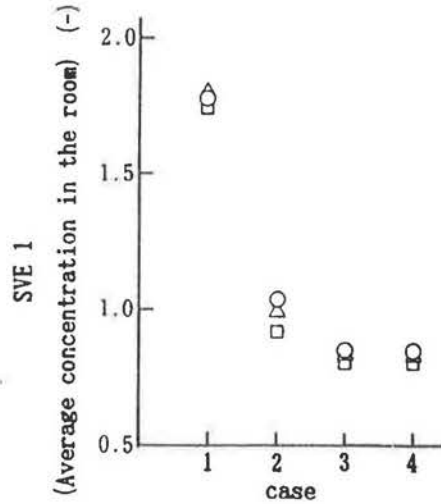


Figure 11 SVE 1 for various layouts of supply-exhaust openings (cases 1 to 4).

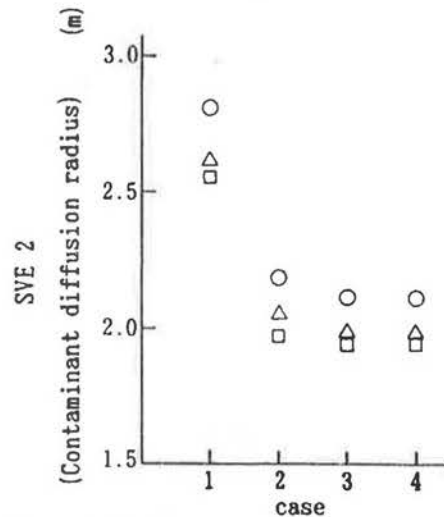


Figure 12 SVE 2 for various layouts of supply-exhaust openings (cases 1 to 4).

### FEATURES OF SVE 3 (CONCENTRATION WHEN CONTAMINANTS ARE GENERATED UNIFORMLY THROUGHOUT THE ROOM)

Figures 13 and 14 show the distribution of SVE 3 for cases 1 and 4 (Types 1 and 4). The concentration distribution where contaminants are generated uniformly throughout the room corresponds to the distribution of the average traveling time of fresh air from the supply outlet. In case 4 (Type 4), where exhaust is completed within one flow unit, the concentration near the ceiling is generally smaller than in case 1 (Type 1).

**TABLE 4**  
**Comparison of Average Concentration in the Room (SVE 1) and Average Diffusion Radius (SVE 2)**

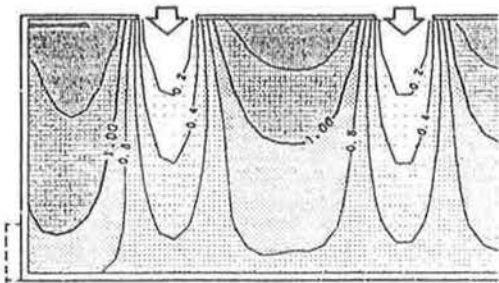
Case No.	Type No.	Source point	Figures	SVE 1	SVE 2
Case 1	Type 1	Point @	Figure 8	1.75	2.81
		Generated uniformly throughout the whole room	Figure 13	0.97	3.33
Case 2	Type 2	Point @	Figure 9	1.05	2.19
Case 3	Type 3	Point @	Omitted (Same as Figure 10)	0.85	2.12
Case 4	Type 4	Point @	Figure 10	0.86	2.11
		Generated uniformly throughout the whole room	Figure 14	0.84	3.37
Case 5	Type 4	Point @ (Top of obstacle)	Figure 15	0.76	2.30
Case 6	Type 4	Point @ (Side of obstacle)	Figure 16	0.87	2.00
Case 7	Type 4	Point @	Figure 7	0.95	2.17
		At supply outlet in the center of room	Figure 7	0.87	2.05
Case 8	Type 4	Point @	Figure 17	1.13	2.34
Case 9	Type 4	Point @	Figure 18	1.06	2.94
Case 10	Type 4	Point @	Figure 19	1.06	2.96

In the case of Type 1, a domain of concentration greater than 1 stretches from the center of the ceiling down the side wall to the floor (Figure 13a). In this portion, fresh air from the supply arrives only after passing over a long route, suggesting that the supplied air is more likely to be contaminated. On the other hand, in the case of Type 4, there is hardly any domain higher than 1 (Figure 14a), showing that fresh air from the supply reaches all points by a relatively short route. As shown in the horizontal section near the ceiling (Figure 14b), the concentration is lower in the area corresponding to the position of the exhaust in the case of Type 4, which suggests that the average traveling time of fresh air to the ceiling is shorter than that of Type 1 (Figure 12b).

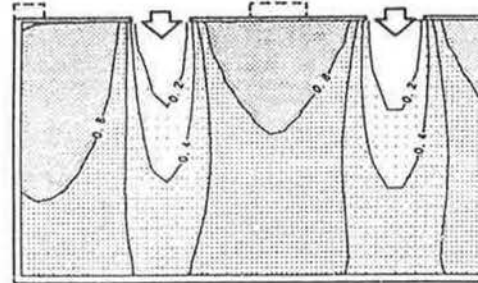
The average concentration in the room (SVE 1) when contaminants are generated uniformly throughout the room is 0.97 for case 1 (Type 1) and 0.84 for case 4 (Type 4), as shown in Table 4. The value is smaller for Type 4, which means that Type 4 is also superior in contaminant exhaust efficiency in the case of uniform contaminant generation in the whole room.

#### EFFECT OF OBSTACLES (COMPARISON OF CASES 5 AND 6)

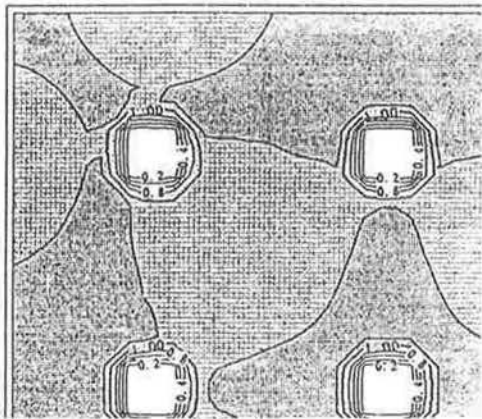
Figure 15 shows the flow and diffusion fields in case 5, where a box-shaped obstacle is placed on the floor just under the supply outlet in the Type 4 room model. The



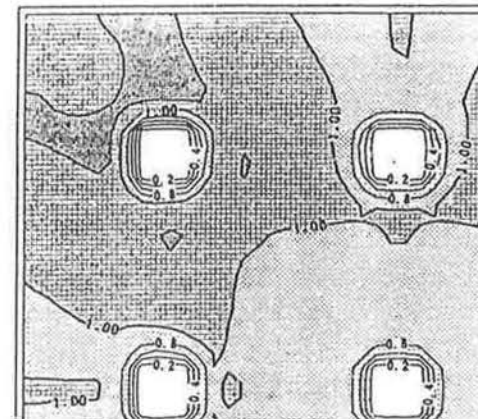
(a) including supply outlets (section)



(a) including supply outlets (section)



(b) near ceiling (plan)



(b) near ceiling (plan)

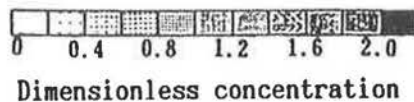
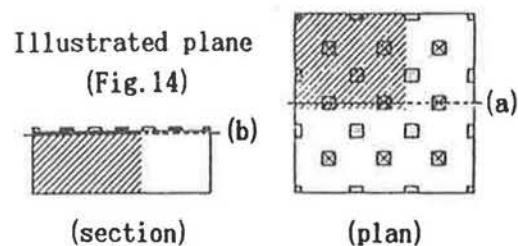
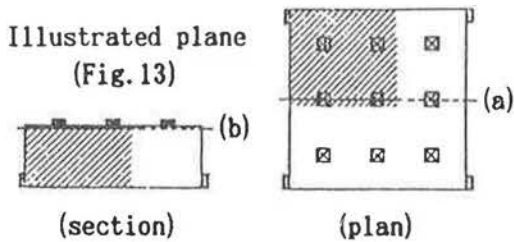


**Figure 13** Contaminant distributions in case 1 (layout: Type 1, source: uniform generation in the whole room).

**Figure 14** Contaminant distributions in case 4 (layout: Type 4, source: uniform generation in the whole room).

supply jet diffuses sideways after colliding with the obstacle (Figure 15a), which results in the formation of an incomplete flow unit in that area. Corresponding to this, contaminants generated above the obstacle diffuse sideways, indicated by a concentration above 0.5 even in the flow unit by the side wall where the concentration in case 4 is below 0.5, resulting in faster contaminant diffusion into the whole room (Figure 15b). On the other hand, in case 6 (Figure 16a), where an obstacle is placed between the supply jets, no significant effect is observed on the flow field compared with case 4 (Figure 10a). In this case, the contaminants generated just under the jet do not

diffuse beyond the obstacle due to the double-shielding effect of the invisible wall of air and the obstacle itself (Figure 16b).

As can be seen from Table 4, in case 5, where the obstacle is placed just under the supply outlet, the average concentration in the room (SVE 1) is 0.76, which is smaller than in cases 4 and 6, where the obstacle is placed between the supply outlets (case 4 [0.86], case 6 [0.87]). This high efficiency in exhausting contaminants is due to the fact that the jet collides with the obstacle and the contaminants are thoroughly dispersed, thus removing the high-concentration domain. However, for case 6, with the



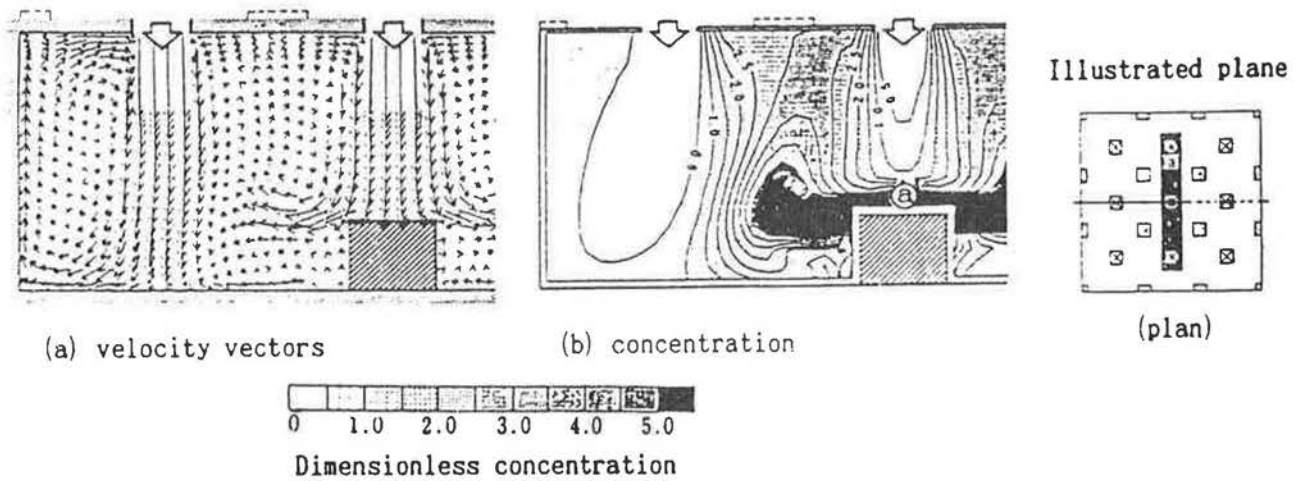


Figure 15 Velocity vectors and contaminant distribution in case 5 (layout: Type 4, an obstacle is placed under supply jets, source: point *a*).

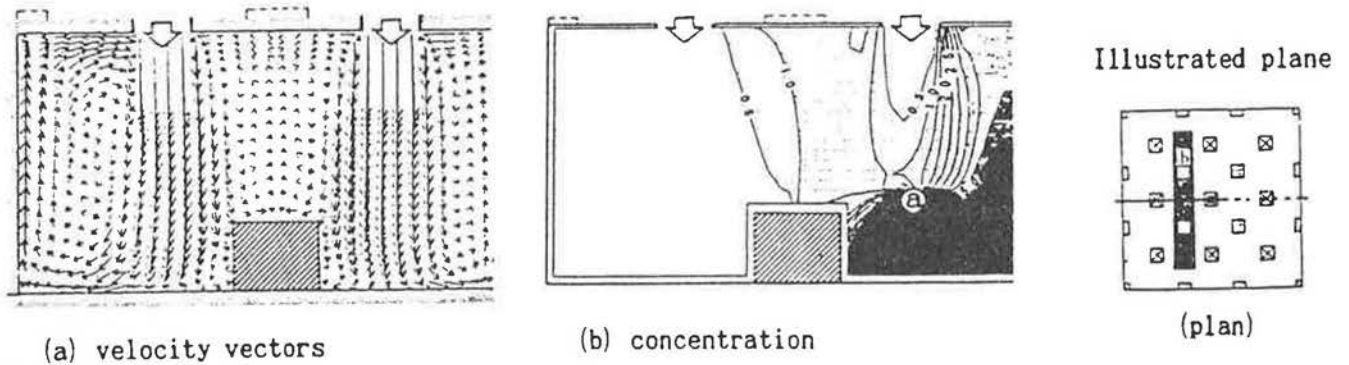


Figure 16 Velocity vectors and contaminant distribution in case 6 (layout: Type 4, an obstacle is placed between supply jets, source: point *a*).

double-shielding effect of the obstacle and the air wall, the average diffusion radius (SVE 2) is 2.0, while it is 2.11 for case 4 and 2.30 for case 5, thus demonstrating the possibility of effective control of contamination via confinement by installing an obstacle. Even with an obstacle, it must be noted that both the average concentration in the room (SVE 1) and the average diffusion radius (SVE 2) are much smaller than in the conventional exhaust-in-wall mode of Type 1 (case 1). Thus, the locally balanced supply-exhaust airflow rate system in the ceiling clearly has a higher contaminant exhaust efficiency than the conventional type.

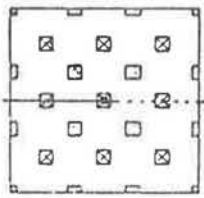
#### EFFECT OF SCATTERING OF SUPPLY-EXHAUST AIR VOLUME DISTRIBUTION

Figure 7c has already shown the results of case 7, where a scatter of about 10% occurs in the flow rate

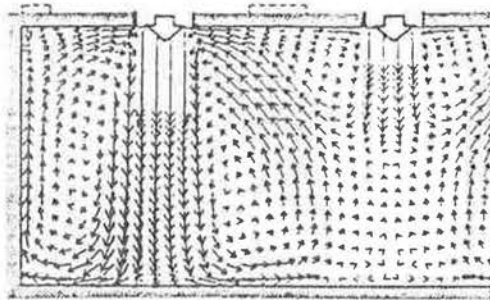
distribution at each supply outlet and exhaust inlet. Such a range of scatter can often be observed in actual conditions. In contrast, Figure 17 shows the results of case 8, where the center supply airflow rate is reduced by 50%; Figure 18 shows case 9, where the center supply airflow is increased by 50%. Of course, this variation of 50% represents an extreme case not likely to be found in actuality. Figure 19 shows the flow and diffusion fields in case 10, where the exhaust airflow of the center flow unit is increased by 50% to correspond with an increase in the center supply airflow in order to attain the air balance in the center flow unit.

Comparing case 4 (Figure 10b) with case 7 (Figure 7b), it might seem that the difference between the contaminant distributions is small. However, as can be seen from Table 4, the average concentration of contaminants in the room (SVE 1) in case 7 is higher, i.e., 0.95 compared with 0.86 in case 4, which indicates a decrease in the efficiency of contaminant exhaust. The diffusion

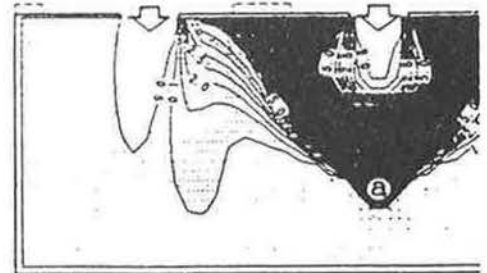
Illustrated plane (Fig. 17, 18, 19)



(plan)



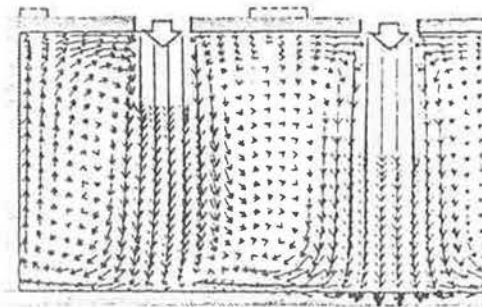
(a) velocity vectors



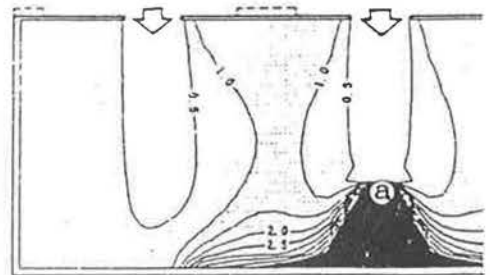
(b) concentration

including supply outlets (section)

Figure 17 Velocity vectors and contaminant distribution in case 8 (layout: Type 4, airflow rate at supply outlet in the center of room is reduced by 50%, source: point @).



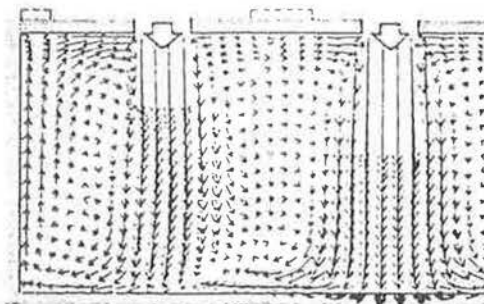
(a) velocity vectors



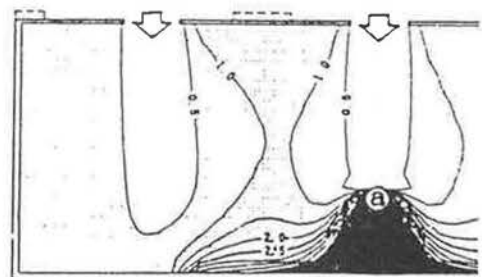
(b) concentration

including supply outlets (section)

Figure 18 Velocity vectors and contaminant distribution in case 9 (layout: Type 4, airflow rate at supply outlet in the center of room is increased by 50%, source: point @).



(a) velocity vectors



(b) concentration

including supply outlets (section)

Figure 19 Velocity vectors and contaminant distribution in case 10 (layout: Type 4, airflow rate at supply outlet in the center of room is increased by 50% and supply-exhaust airflow rate is balanced by four exhaust inlets around it; source: point @).

radius (SVE 2) in case 7 is also somewhat larger, i.e., 2.17 compared with 2.11 in case 4, showing a less limiting effect on contaminant diffusion as well. However, SVE 1 and SVE 2 in case 7 are smaller than their values for the Type 2 clean room (case 2)—1.05 and 2.19, respectively—with the ventilation efficiency being better than in case 2.

In case 8, where the supply airflow at the center of the room is drastically reduced, the jet from the center supply outlet does not reach the floor and thereby the jets on the right and left sides invade the area under the center supply outlet, forming a strong slanting rising stream (Figure 17a). Correspondingly, as the contaminants are convected by this strong rising stream toward the ceiling and are exhausted, no concentration domain greater than 1 is observed near the floor. However, as shown in Table 4, case 8 has a higher average concentration of contaminants in the room (SVE 1) compared to cases 4 through 10, which indicates a decrease in the efficiency of contaminant exhaust. The diffusion radius (SVE 2) also is larger, i.e., 2.34 compared with 2.11 in case 4.

In case 9, the supply-exhaust rate is forced out of balance by increasing the supply rate at the center supply outlet, and in case 10, the supply-exhaust flow rate is balanced by matching the exhaust flow rate with the increased supply flow rate at the center supply outlet. In these cases, flow and diffusion fields are approximately the same regardless of the changes in exhaust flow rates at the center flow unit (Figures 18 and 19). It may be concluded that a large scattering in the supply airflow rate distribution, as in these cases, decreases the possibility of limiting the diffusion to a single flow unit, even if the supply-exhaust airflow is balanced in each flow unit. As can be seen from Table 4, the ventilation efficiency of exhausting contaminant (SVE 1) in cases 7 through 10 apparently decreases in comparison with case 4. In particular, in cases 8 through 10, the contaminant concentration along the wall side is larger than 0.5. However, compared with the average concentration in the conventional flow-type clean room in case 1, cases 9 and 10 yield much smaller values, indicating that the ventilation efficiency is still higher.

## CONCLUSIONS

1. Compared with a conventional ventilation system, the locally balanced supply-exhaust airflow rate system allows more efficient exhaust of contaminants and less extensive diffusion in a room.
2. When supply and exhaust rates are locally balanced in each flow unit, minor changes in the location of exhaust inlets have little effect on either airflow or contaminant diffusion performance.
3. When scatters of  $\pm 10\%$  were given to the flow rates at the supply and exhaust openings, ventilation efficiency was slightly decreased compared to conditions when supply and exhaust airflow rates were

precisely balanced. However, this effect was small and the performance of the locally balanced supply-exhaust airflow rate system was maintained.

4. The effect of an obstacle on both flow and diffusion fields is larger when it is located just under the jet flow than when it is located between supply jets. When an obstacle is located just under the supply jet, the potential for restricting diffusion to within the single flow unit is decreased.
5. A large imbalance between supply and exhaust due to excessive air supply or excessive air exhaust per flow unit decreases ventilation efficiency by decreasing the potential for restricting diffusion to within a single flow unit.
6. Even if the supply-exhaust rate per flow unit is balanced, when those values are not uniform and deviations among all the flow units are large, there is more diffusion of contaminants than when the air supply-exhaust rates are uniform.

## ACKNOWLEDGMENT

This study has been partially supported by a grant-in-aid for scientific research from the Japanese Ministry of Education, Culture, and Science. The calculations of diffusion fields were conducted by the engineering work station of DN 10000 courtesy of HP.

## NOMENCLATURE

$C_\mu, C_1,$ and $C_2$	= empirical constants in k- $\epsilon$ turbulence model (cf. Table 2)
$C$	= mean contamination concentration
$C_s$	= contamination concentration source term
$E$	= empirical constant in log law, 9.0 in case of smooth wall
$h$	= length from the wall surface to the center of the adjacent cell
$k$	= turbulent kinetic energy
$k_o$	= turbulent kinetic energy given at supply outlet
$\ell$	= length scale of turbulence
$\ell_o$	= length scale of turbulence given at supply outlet
$P$	= mean pressure
SVE	= scale of ventilation efficiency
$U_i, U_j$	= components of mean velocity vector
$\epsilon$	= turbulence dissipation rate
$\kappa$	= von Karman constant, 0.4
$\rho$	= fluid density
$\nu_t$	= eddy kinematic viscosity
$\sigma_1, \sigma_2,$ and $\sigma_3$	= turbulence Prandtl/Schmidt number of $k, \epsilon, C$ (cf. Table 2)

**TABLE 5**  
**Experimental Conditions**

Experiment No.	Type No.	Air Supply Condition	Obstacle	Position of supply outlet generating tracer
1	Type 1	Uniform* <sup>1</sup>	Nothing	Ⓐ
2	Type 4	Uniform	Nothing	Ⓐ
3	Type 4	Uniform	Nothing	Ⓑ
4	Type 4	Uniform	Nothing	Ⓒ
5	Type 4	Uniform	One obstacle is installed in the center of room as shown in Figure 20	Ⓐ
6	Type 4	Air flow rate at supply outlet in the center of room is reduced by 62 %	Nothing	Ⓐ

NOTE : \*1 There are scatterings in the air flow rate in reality as shown in Figure 22, although uniformity of air flow rate is aimed at.

- 1) Supply air velocity is 6.0m/s, Reynolds number of supply jet is 40000.
- 2) Tracer is injected at the upstream of supply outlet (the distance about 6 times the outlet width). The scattering of concentration at the outlet face is within  $\pm 10\%$  on the measurement of tracer concentration dividing supply outlet into 9 meshes equally.
- 3) The injection rate of tracer is 50 cc/s per air volume of 0.5 m<sup>3</sup>/s and the average concentration of all exhaust inlets is 100 ppm.

## REFERENCES

- Kato, S., and S. Murakami. 1988. New ventilation efficiency scales based on spatial distribution of contaminant concentration aided by numerical simulation. *ASHRAE Transactions* 94(2): 309-330.
- Kato, S., S. Murakami, and Y. Kondo. 1991. Numerical simulation of 2-D air flow with and without buoyancy by means of ASM. Unpublished paper.
- Murakami, S., and H. Komine. 1980. Measurement of three components of turbulent flow with tandem hot-wire probe. *Transactions of Architectural Institute of Japan* 297: 59-69.
- Murakami, S., S. Kato, and Y. Suyama. 1987. Three-dimensional numerical simulation of turbulent airflow in ventilational room by means of a two-equation model. *ASHRAE Transactions* 93(2): 621-642.
- Murakami, S., S. Kato, and Y. Suyama. 1988. Numerical and experiment study of turbulent diffusion fields in conventional flow-type clean room. *ASHRAE Transactions* 94(2): 469-493.
- Murakami, S., S. Kato, and Y. Suyama. 1989. Numerical study of diffusion field as affected by arrangement of supply and exhaust openings in conventional flow-type clean room. *ASHRAE Transactions* 95(2): 113-127.
- Murakami, S., S. Kato, and Y. Suyama. 1990a. Numerical study of flow and contaminant diffusion fields as affected by flow obstacles in conventional flow-type clean room. *ASHRAE Transactions* 96(2): 343-355.
- Murakami, S., S. Kato, and Y. Kondo. 1990b. Examining k- $\epsilon$  EVM by means of ASM for a 3-D horizontal buoyant jet in enclosed space. *Engineering Turbulence Modelling and Experiments*, W. Rodi and E.N. Ganic, eds., 205-214. Amsterdam: Elsevier.



## APPENDIX

### MODEL EXPERIMENTS

Figure 20 shows the types of room models used. They are models of conventional flow-type clean rooms. Type 1 is an ordinary model where the exhaust openings are installed in the wall near the floor. Type 4 is a room model with the locally balanced supply-exhaust ventilation system in the ceiling. The rate of supply and exhaust airflow in each flow unit is designed to be balanced to a certain accuracy.

### SUMMARY OF MEASUREMENTS

Figure 21 is an outline of the model used for experiments, and Table 5 gives the experimental conditions. The experiments were carried out using isothermal inflow jets. The flow velocity was measured three-dimensionally using a tandem-type hot-wire anemometer (Murakami et al. 1980), and the tracer gas ( $C_2H_4$ ) concentration was monitored using a flame ionization detector (FID). Concentration and velocity were measured at the same measuring locations. The supply-exhaust airflow rate was calculated from the measured value of flow velocity using a thermistor anemometer.

### RESULTS

#### Scattering of Air Volume Rate Distribution for Supply and Exhaust Openings

Figure 22 shows the scattering in airflow rates at the supply outlets and exhaust inlets of Types 1 and 4. In both cases the scatter falls within the range of  $\pm 15\%$ .

### FLOW FIELDS

Figure 23 shows the velocity vectors in the vertical section at the center of Types 1 and 4. As shown in Figure 23b, the airflow pattern is approximately symmetric, so only one side of the symmetry is denoted. The formation of a flow unit from each supply jet and the rising stream around it is similar in both cases. Comparing the flow fields of both cases in detail, the following differences can be found.

1. In the case of the wall exhaust mode (Figure 23a, Type 1), the rising airstream between the supply outlets comes to a standstill at about one-third of the room height.
2. In the case of the locally balanced supply-exhaust ventilation system in the ceiling (Figure 23b, Type 4), the rising airstream between the supply outlets reaches the ceiling.

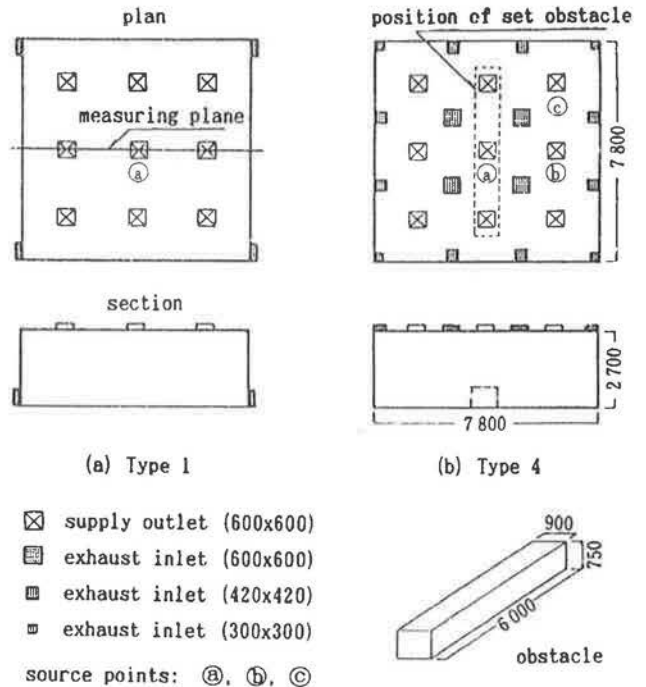
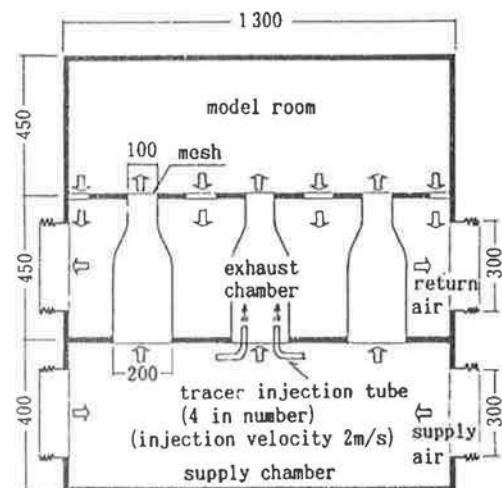


Figure 20 Plans and sections of room models (unit: mm).

3. In the case where an obstacle (Figure 20) is placed just under the ceiling supply outlet (Figure 23c, Type 4, experiment 5), the supply jet, after striking the top of the obstacle, forms strong convective flows to the side.
4. If the supply airflow at the center of the room is reduced by 62% (Figure 23d, Type 4, experiment 6), the supply jet does not reach the floor since there is interference from the jets of the supply outlets around it.



NOTE: Room model is made upside down for the convenience of measurement.

Figure 21 Experimental model with supply and exhaust systems (unit: mm).

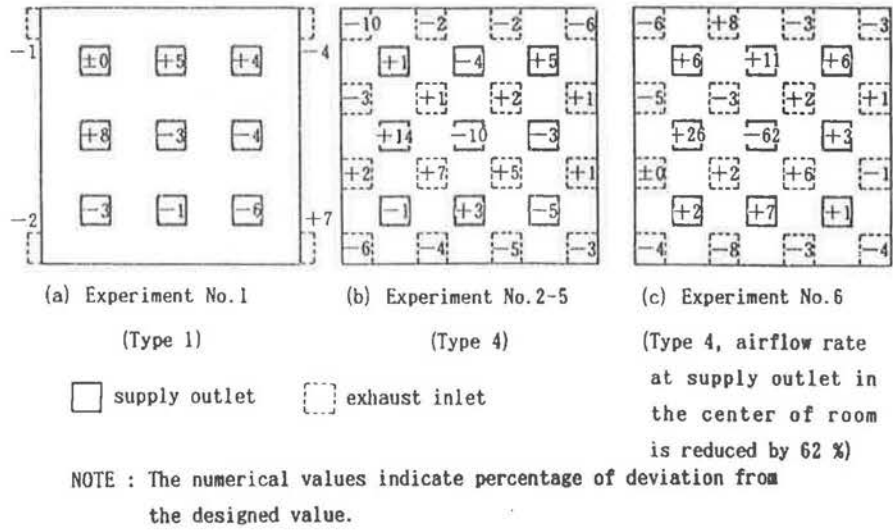


Figure 22 Scattering of supply-exhaust air volume (unit: %).

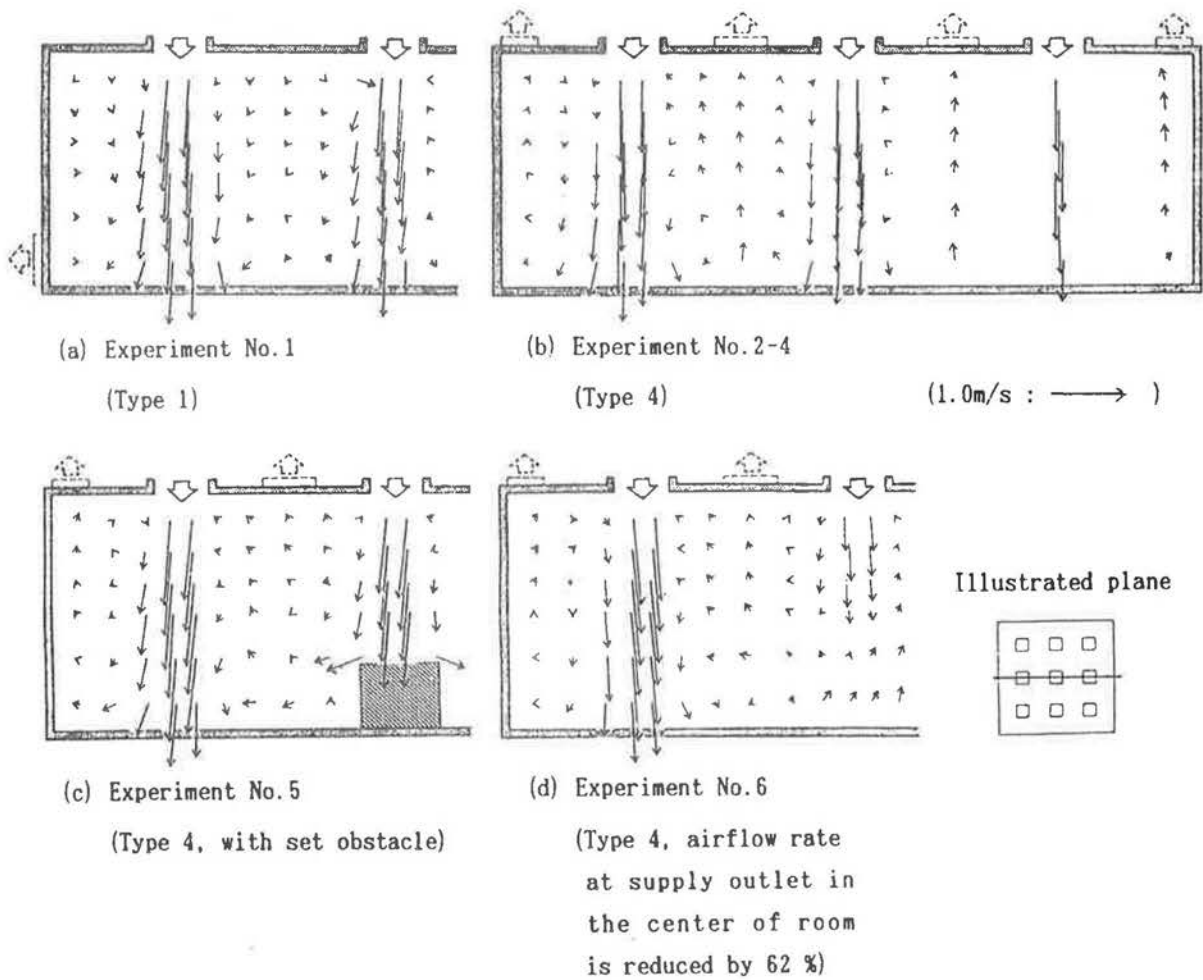


Figure 23 Velocity vectors by measurements.

## DIFFUSION FIELDS

The concentration distribution of contaminants in a vertical section when contaminants are discharged from supply outlet (a) (Figure 20) are compared for Types 1 and 4. The concentration is made dimensionless by dividing by the complete mixing concentration (nominal concentration, average concentration of all exhaust inlets).

### Comparison between Wall Exhaust Mode and Locally Balanced Supply-Exhaust Ventilation System in the Ceiling

In Type 1, there are many areas with a dimensionless concentration of more than 1 (Figure 24a, experiment 1). In particular, there is a domain where the concentration is rather high (dimensionless concentration of about 2.0) near the top of the wall. In Type 4, the dimensionless concentration near the wall is less than 1 (Figure 24b, experiment 2). Thus the restricting effect on contaminant

diffusion to within the flow unit where the contaminants are generated is confirmed.

### Effect of Obstacles

In Type 4 there is no obstacle (Figure 24b, experiment 2), and the dimensionless concentration in the domain between the supply outlet and the wall is less than 1. When an obstacle is put in place (Figure 24c, experiment 5), the concentration at the same area rises above 1 over a wide area.

### Imbalance of Supply-Exhaust Airflow in Flow Unit

If the airflow at the center supply outlet is reduced by 62 % (Figure 24d, experiment 6), a large, higher concentration domain is formed under the supply outlet (dimensionless concentration greater than 4.0). It is caused by the interference of diffusion from the stronger jets supplied from the supply outlets nearby. However, no

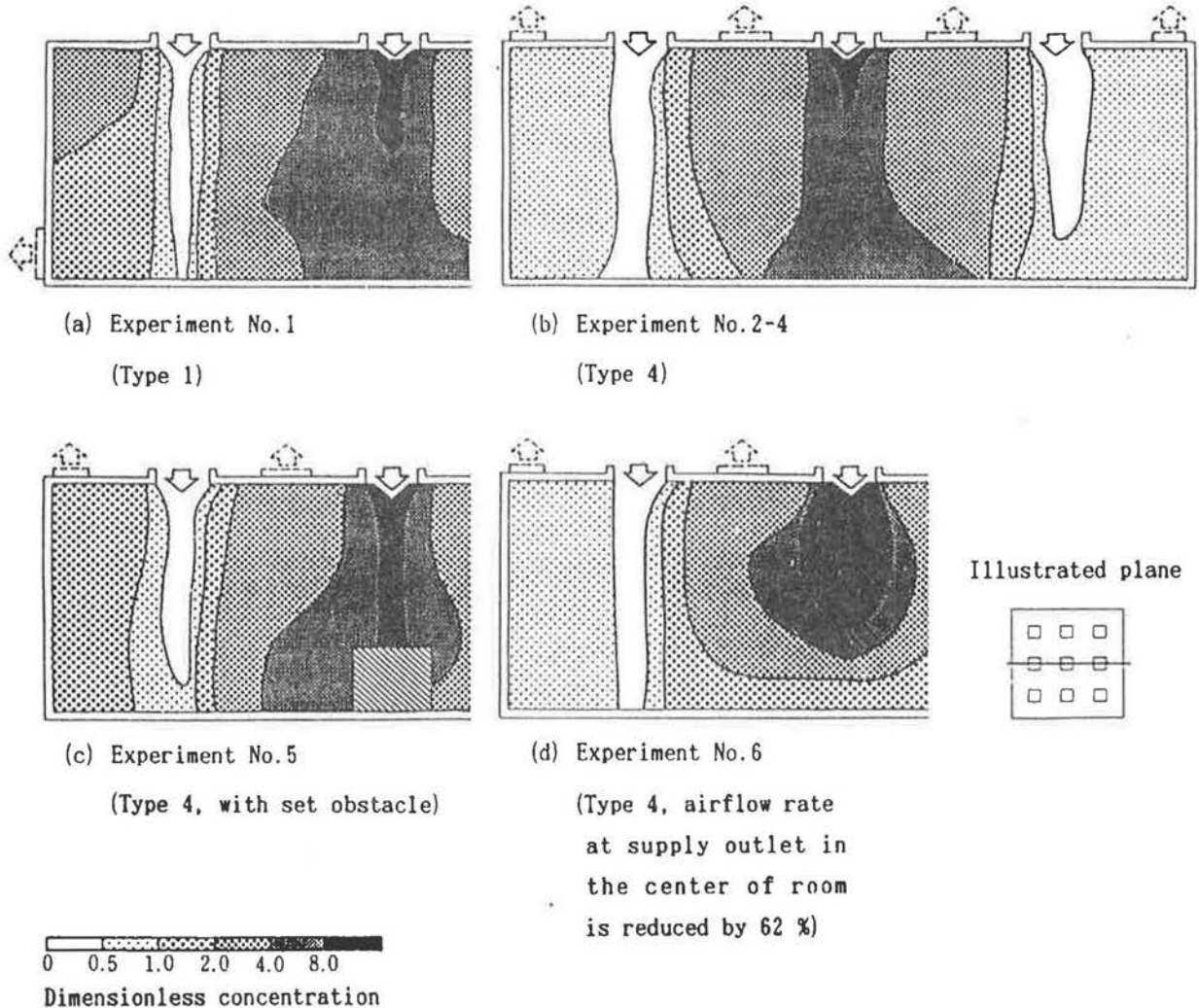


Figure 24 Contaminant distributions by measurements.

change in the cleanliness of other flow units was observed.

### Method of Evaluating Ventilation Efficiency by Experiment

### EXAMINATION OF VENTILATION EFFICIENCY USING EXPERIMENTAL METHOD

By injecting contaminants into supply outlets (a), (b), and (c) in Type 4, the ventilation efficiency (efficiency of contaminant exhaust) was examined, as shown in Figure 25.

To thoroughly examine the ventilation efficiency of the room, the best method is to use the SVE (scale of ventilation efficiency). However, it is difficult to calculate this from measured data, so the evaluation based on SVEs has not yet been performed. Thus, the ventilation efficiency of the room is evaluated on the basis of the rate of contaminant exhaust from each exhaust opening, as

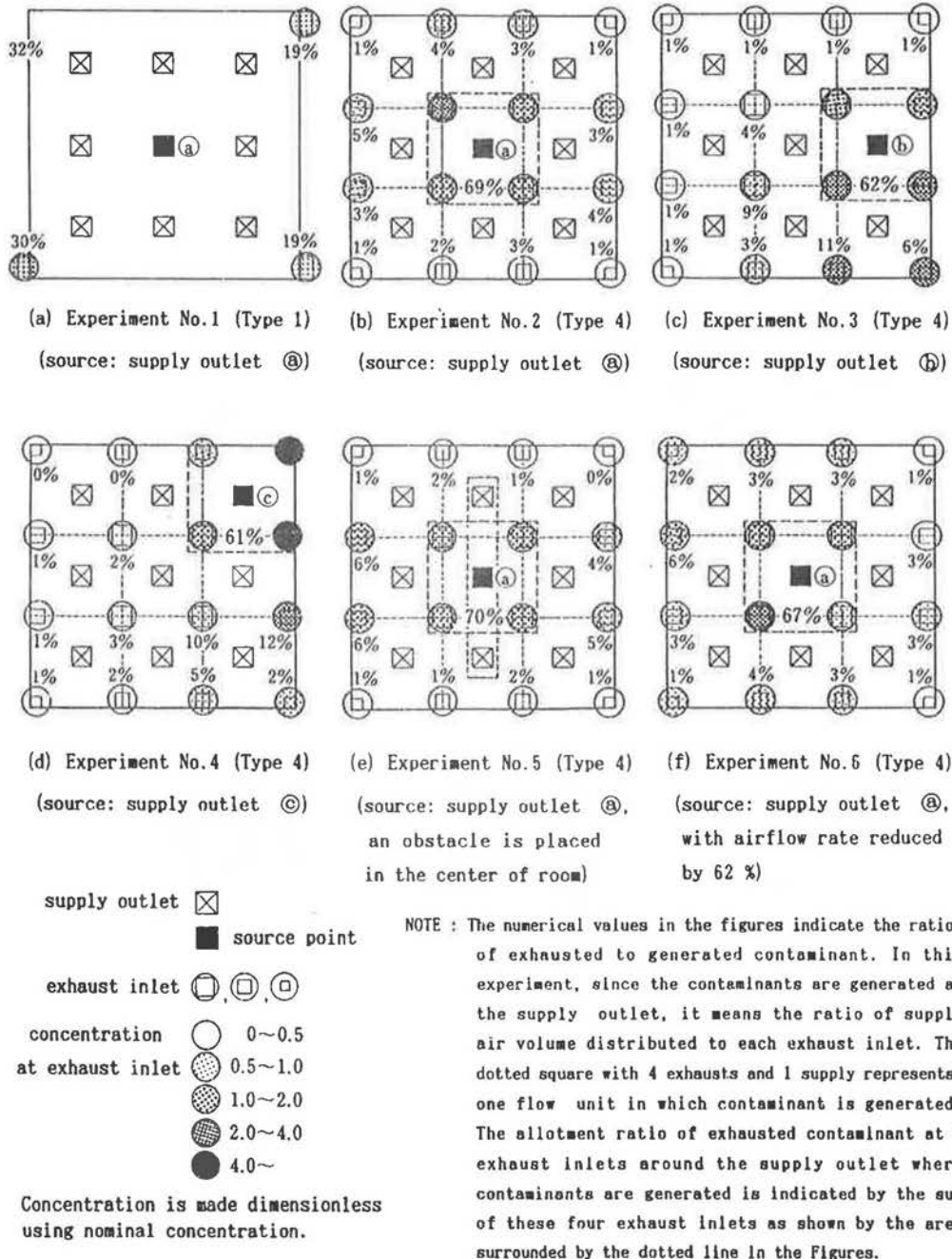


Figure 25 Allotment ratio of contaminant exhaust.



calculated from the exhaust airflow and contaminant concentration at each exhaust opening.

### Contaminant Exhaust Ratio

The ratio of contaminant exhausted from each exhaust inlet to contaminant generated is defined as the allotment ratio. Figure 25 shows the sum of the allotment ratios for four exhaust inlets around contaminant sources (a), (b), and (c) of a flow unit. If the contaminants have been completely mixed with air and diffuse uniformly throughout the room, the allotment ratio should be 44% ( $= 4/9$ ) (a), 33% ( $= 3/9$ ) (b), and 25% ( $= 2.25/9$ ) (c), respectively, from the air volume ratio of the exhaust inlets. As shown in Figure 25, however, the values are actually considerably higher, i.e., 67% to 70% (a) (Figures 25b, 25e, and 25f), 62% (b) (Figure 25c), and 61% (c) (Figure 25d), respectively. Thus, contaminant diffusion appears to be significantly restricted locally. Further, in the case of the wall exhaust system (Type 1), if contaminants are injected through supply outlet (a), for example, they diffuse equally to exhaust inlets in the four corners (19% to 32% each in the results of experiment 1, Figure 25a). Therefore, it can be concluded that Type 4 is more effective from the viewpoint of ventilation efficiency, since it confines the diffusion of contaminants, and the contaminants generated

are exhausted effectively from an area as near to the source as possible.

Regarding cases where an obstacle exists (Figure 25e, experiment 5) and the supply-exhaust air volume is not balanced (Figure 25f, experiment 6), the results obtained do not differ much from those of experiment 2 (Figure 25b).

The results of these experiments demonstrate that the concentration at the exhaust inlets correlates well with the distance from the contaminant source. The effect of an obstacle and imbalance in the supply-exhaust airflow is very small. That is, the ventilation efficiency from the viewpoint of the allotment ratio is not affected by an obstacle or by an imbalance in the airflow rate.

This may be because, in the locally balanced supply-exhaust ventilation system in the ceiling, (1) large-scale recirculating flow throughout the room cannot be formed, (2) many of the contaminants generated in one flow unit are exhausted at its own exhaust inlets by means of flow convection, and (3) the contaminants that diffuse to neighboring flow units due to turbulent diffusion or an imbalance in the supply-exhaust flow rate of that flow unit are exhausted at the inlets of the neighboring flow units. Therefore, the possibility is relatively small that they will be transported to other flow units.